# How COVID-19 related policies reshaped organic aerosol

2 source contributions in Central London

3

14

4 Gang I. Chen<sup>1</sup>\*, Anja H. Tremper<sup>1</sup>, Max Priestman<sup>1</sup>, Anna Font<sup>2</sup>, and David C. Green<sup>1,3</sup>

<sup>1</sup>MRC Centre for Environment and Health, Environmental Research Group, Imperial College
 London, 86 Wood Lane, London, W12 0BZ, UK

<sup>2</sup>IMT Nord Europe, Europe, Institut Mines-Télécom, Univ. Lille, Centre for Education, Research
 and Innovation in Energy Environment (CERI EE), 59000 Lille, France

<sup>3</sup>HPRU in Environmental Exposures and Health, Imperial College London, 86 Wood Lane,
 London, W12 0BZ, UK

15 \*Correspondence to: Gang I. Chen (gang.chen@imperial.ac.uk)

### 16 Abstract

17

18

19

20

21

22

23

24

25

26

27

28

29

30

31

32

33

34

35

36

Organic aerosol (OA), a major component of submicron particulate matter (PM<sub>1</sub>), has significant impacts on both human health and climate. Quantifying its sources is therefore crucial for developing effective mitigation strategies. Positive matrix factorisation (PMF) applied to aerosol chemical speciation monitor (ACSM) mass spectral data offers a robust approach for quantifying OA sources. A year-long study of ACSM data from London's Marylebone Road monitoring station during the COVID-19 pandemic provides insights into the impact of lockdown and the Eat Out To Help Out (EOTHO) scheme, which offered support to the hospitality industry during the pandemic, on PM composition and OA sources. Five OA sources were identified including hydrocarbon-like OA (HOA, traffic-related, 11% to OA), cooking OA (COA, 20%), biomass burning OA (BBOA, 12%), more-oxidized oxygenated OA (MO-OOA, 38%), and less-oxidized oxygenated OA (LO-OOA, 21%). Lockdown significantly reduced HOA (-52%), COA (-67%), and BBOA (-42%) compared to their pre-COVID levels, while EOTHO doubled COA (+100%) compared to the postlockdown period. However, MO-OOA and LO-OOA were less affected, as these primarily originated from long-range transport. This research has demonstrated the importance of commercial cooking as a significant source of OA (20%) and PM<sub>1</sub> (9%) in urban areas. The coemission of BBOA with COA observed in Central London showed a similar diurnal cycle and response to the EOTHO policy, indicating that cooking activities might be currently underestimated and contribute to urban BBOA. Therefore, more effort is required to quantify this source and develop targeted abatement policies to mitigate emissions as currently limited regulation is in force.

### 1 Introduction

38

39

40

41

42

43

44

45

46

47

48

49

50

51

52

53

54

55

56

57

58

59

Atmospheric particulate matter (PM) are tiny particles suspended in the air, which impact the climate directly and indirectly (IPCC, 2021; Seinfeld et al., 2006), and cause adverse human health effects (Kelly and Fussell, 2012; World Health Organization, 2021). The PM present in urban areas, such as London, is emitted directly or indirectly from a wide range of natural and anthropogenic sources, can be changed through atmospheric reactions and remain airborne for many days. It is consequently a complex mixture including inorganic species (metals, minerals, black carbon, nitrate, sulphate, etc.) and thousands of organic compounds whose origins remain too complicated to fully quantify. PM<sub>2.5</sub> (PM with aerodynamic diameter smaller than 2.5 µm) is strongly associated with increased risks of cardiovascular and respiratory related mortalities and hospital admissions (Dominici et al., 2006; Joo et al., 2024; Pye et al., 2021; Wei et al., 2022, 2024). Some studies (Lippmann et al., 2013; UK Health Security Agency (UKHSA), 2022) have begun to demonstrate that some PM constituents and sources have stronger associations with a range of health metrics, including mortality, morbidity, and toxicities although the evidence remains inconsistent (Kelly and Fussell, 2012; Liu et al., 2023; Vasilakopoulou et al., 2023). With 99% of the urban population in Europe exposed to PM<sub>2.5</sub> concentrations exceeding the WHO air quality guideline (European Environment Agency, 2024; World Health Organization, 2021), delivering clean air is a target for European and international governments according to the EU air quality directive (European Union, 2024). However, delivering publicly acceptable policies to improve air quality remains challenging (Mebrahtu et al., 2023; Oltra et al., 2021). Targeting the sources of PM that are most health-relevant could be a more cost-effective (Wu et al., 2023), more easily communicated and more publicly acceptable approaches (Pinakidou, 2025) to improve public

60 health. It is therefore important to better quantify the sources of PM and understand how they 61 respond to policy interventions. 62 The COVID-19 pandemic is a natural experiment to assess the impact of policies which, while not 63 aiming to reduce PM<sub>2.5</sub> concentrations, significantly restricted social and economic activities and 64 consequently reduced emissions. During the UK national lockdown, people were ordered to stay 65 at home, and all non-essential businesses were closed, including pubs, cafes and restaurants from the end of Mar 26<sup>th</sup>, 2020. Non-essential shops were allowed to open from Jun 15<sup>th</sup>, and the first 66 national lockdown came to an end on Jun 23<sup>rd</sup>, 2020. However, pubs, restaurants, and cafes were 67 only allowed to open from July 4<sup>th</sup>, 2020. The UK recorded a 2.5% drop in Gross Domestic Product 68 69 (GDP) in the first quarter of 2020, partly as people reduced their own activity prior to national lockdown. This accelerated to a 19.8% fall in GDP in April to June 2020 and household spending 70 71 fell by over 20% over this period, the largest quarterly contraction on record, which was driven by 72 falls in spending on restaurants, hotels, transport, and recreation (ONS, 2022). The UK 73 Government Eat Out to Help Out (EOTHO) Scheme is examined specifically in this study as it 74 influenced emissions from the commercial cooking sector. It was designed to help the hospitality 75 industry recover from the financial impact of the national lockdown, offering a 50% meal discount up to a maximum of £10, which operated Mon to Wed, Aug 3<sup>rd</sup> to Aug 31<sup>st</sup>, 2020. 76 77 While the impact of these lockdown policies on some air quality metrics was smaller than expected 78 given the large change in emissions (Shi et al., 2021), the abrupt nature of the intervention ensures 79 it is easier to detect than other air quality policies that are more incremental in nature (Mudway et 80 al., 2019). Some studies have investigated the lockdown impacts on chemical composition and 81 sources of PM, which mainly focused on cities in China (Hu et al., 2022; Tian et al., 2021; Xu et 82 al., 2020), a kerbside site in Toronto, Canada (Jeong et al., 2022), and an urban background site in

84

85

86

87

88

89

90

91

92

93

94

95

96

97

98

99

100

101

102

103

104

105

Paris, France (Petit et al., 2021). These studies all resolved primary sources including traffic related emissions, biomass burning emissions from residential heating, cooking emissions (except Paris), and secondary sources from PMF analysis on organic aerosol (OA). Traffic and cooking emissions appeared to decrease during the lockdown in all sites, while biomass burning predominately from residential heating sources in Chinese cities increased as result of remote work and rather early lockdown measures (Jan-Feb 2020) compared to France. Secondary organic aerosol (SOA) showed a more complex phenomenon given its abundance in organic components and dynamic spatiotemporal conditions. Overall, the lockdowns resulted in decreased SOA in both northwest cities in China (Tian et al., 2021; Xu et al., 2020) and Paris (Petit et al., 2021) due to lower primary emissions, and therefore fewer SOA formation products. However, Beijing experienced a large increase in SOA concentrations due to increased fossil fuel and biomass burning emissions, longrange transport influences as well as favourable meteorological conditions (high RH, low wind speed and low boundary layer height) for SOA formation during the lockdown period (Hu et al., 2022). Therefore, the lockdown effects on the SOA were dependent on the abundance of primary emissions, long-range transported air masses, and meteorological conditions. To date, there are few studies that investigate how COVID-related policies could have impacted PM chemical composition and sources. Petit et al. (2021) and Gamelas et al. (2023) are the only two studies in Europe. The unique COVID-related policies in the UK therefore provide a rare opportunity to investigate the impacts these policies had on chemical composition and OA. We used highly time resolved measurements from an air quality supersite located in the Central London from 2019 to 2020, and advanced source apportionment approaches to quantify the PM composition and OA sources before, during and after the UK national lockdown and EOTHO scheme. This study provides valuable insight into PM sources and composition in a global mega city and how air quality responds to abrupt changes in emissions from different sources. Importantly, it helps to establish the importance of cooking as a source of PM and uniquely associates biomass burning organic aerosol with commercial cooking emissions. This provides crucial information to policy makers as they attempt to reduce exposure to air pollution in urban areas.

# 2 Methodology

#### 2.1 Air quality monitoring supersite in Central London

The London Marylebone Road supersite (MY, 51.52 N, -0.15 E) is a kerbside air quality monitoring site, one meter away from a busy 6-lane road in CentralLondon. It is a well-established air quality supersite that has consistently generated high-quality air pollution data since 1997 including mass concentration of bulk PM<sub>1</sub>, PM<sub>2.5</sub>, and PM<sub>10</sub>, as well as PM composition including black carbon, heavy metals, nitrate (NO<sub>3</sub>), sulphate (SO<sub>4</sub>), ammonium (NH<sub>4</sub>), OA, Chloride (Cl), etc. More details of this site can be found at https://uk-air.defra.gov.uk/networks/site-info?site id=MY1.

#### 2.2 Instrumentations

Quadrupole ACSM (Q-ACSM, Aerodyne, Ltd., Ng et al. (2011)) with a standard vaporizer provides 30-min mass loadings of chemical species within non-refractory submicron aerosol (NR-PM<sub>1</sub>), including NH<sub>4</sub>, NO<sub>3</sub>, SO<sub>4</sub>, Cl, and OA. Sampled particles are focused into a narrow beam using the aerodynamic lens and impacted on a filament surface at 600 °C, where the NR-PM<sub>1</sub> is vaporised and ionised instantly by an electron impact source (70eV). These ions are detected by the RGA quadrupole mass spectroscopy to provide a mass spectrum of NR-PM<sub>1</sub> up to a mass-to-charge ratio (*m/z*) of 148 Th. The mass concentration of different chemical species are calculated

using the fragmentation table developed by Allan et al. (2004), updated for Cl following suggestions provided by Tobler et al. (2020), and a composition-dependent collection efficiency (CDCE) correction suggested by Middlebrook et al. (2012) by following the ACTRIS standard operation procedure (<a href="https://www.actris-ecac.eu/pmc-non-refractory-organics-and-inorganics">https://www.actris-ecac.eu/pmc-non-refractory-organics-and-inorganics</a>). With co-located black carbon (BC) measurement using a PM<sub>2.5</sub> cyclone with AE33 (Aerosol Magee Scientific, Ltd.) and PM<sub>1</sub> measurements using FIDAS (Palas, GmbH), we conducted the mass closure for fine particles measurements. The sum of NR-PM<sub>1</sub> and BC (in PM<sub>2.5</sub>) reproduces PM<sub>1</sub> concentrations well, with a slope of 1.13 and an R<sup>2</sup> of 0.73 (Fig. S1).

### 2.3 Sampling periods and COVID-related policies

PM<sub>1</sub> chemical composition from Aug 1<sup>st</sup>, 2019 to Oct 22<sup>nd</sup>, 2020, was analysed as this covered the first lockdown period (Mar 26<sup>th</sup>–23 Jun 23<sup>rd</sup>, 2020) and the EOTHO Scheme (Mon-Wed during from Aug 3<sup>rd</sup> to Aug 31<sup>st</sup>, 2020, Table 1). In order to isolate the seasonal effects on the PM chemical composition and OA sources from the COVID-related policies, we further split the data based on seasons (Table 1).

Table 1 Dates of the COVID-related policies in London

	Date
Summer	Aug 1 <sup>st</sup> –Aug 31 <sup>st</sup> , 2019
Fall	Sep 1 <sup>st</sup> –Nov 30 <sup>th</sup> , 2019
Winter	Dec 1 <sup>st</sup> , 2019–Feb 28 <sup>th</sup> , 2019
Spring	Mar 1 <sup>st</sup> –Mar 25 <sup>th</sup> , 2020
Spring	Mar 26 <sup>th</sup> –May 31 <sup>st</sup> , 2020
Summer	Jun 1 <sup>st</sup> –Jun 23 <sup>rd</sup> , 2020
	Fall Winter Spring Spring

	Pre-EOTHO	Jun 24 <sup>th</sup> –Aug 2 <sup>nd</sup> , 2020
Post-Lockdown	ЕОТНО	Aug 3 <sup>rd</sup> –Aug 31 <sup>st</sup> , 2020
	Post-EOTHO	Sep 1 <sup>st</sup> –Oct 22 <sup>nd</sup> , 2020

#### 2.4 Source apportionment

143

144

145

146

147

148

149

150

151

152

153

154

155

156

157

158

159

160

161

Source apportionment is a common but powerful approach to identifying and quantifying the emission sources and atmospheric constituents of PM based on measurements. As the sources of inorganic species (black carbon, ammonium, nitrate, chloride, sulphate, etc.) are relatively wellstudied, most of the studies are focused on deconvoluting the sources of OA, which contains thousands of compounds. Positive matrix factorization (PMF) is one of the receptor models that is widely utilized in the field to conduct source apportionment analysis (Jimenez et al., 2009; Zhang et al., 2007). Typically, an Aerodyne aerosol mass spectrometer (AMS, Aerodyne Ltd., USA, Jayne et al., 2000) is used to measure the time series of both inorganic and organic species of nonrefractory PM, in which, organic mass spectra are used for PMF analysis. However, operating an AMS is labour-intense and expensive. In contrast, the aerosol chemical speciation monitor (ACSM, Aerodyne, Ltd., Fröhlich et al., 2013; Ng et al., 2011) has been designed for long-term monitoring purposes with less maintenance and lower capital cost, which has gained popularity across Europe (Chebaicheb et al., 2024; Chen et al., 2022; Laj et al., 2024) and the U.S. (https://ascent.research.gatech.edu/, (Hass-Mitchell et al., 2024; Joo et al., 2024)). Chen et al. (2022) demonstrated a robust protocol to conduct advanced PMF analysis on long-term ACSM datasets, which delivers high-quality and consistent source apportionment results. This study follows this standardized protocol to resolve the OA sources in London by implementing advanced PMF techniques.

163

164

165

166

167

168

169

170

171

172

173

174

175

176

177

178

179

180

181

182

183

Advanced source apportionment approaches have been used in this study, including rolling positive matrix factorization (PMF), ME-2 with random a-value approach, bootstrap and criteriabased selections (Canonaco et al., 2021; Chen et al., 2022). The standardized protocol of rolling PMF as presented in Chen et al. (2022) was used to ensure high-quality and comparable sources of OA were retrieved in London. Specifically, PMF was firstly done on four different seasons as suggested in Chen et al. (2022) to determine the optimum number of factors. A total of 5 OA factors were identified: hydrocarbon-like OA (HOA), cooking-like OA (COA), biomass burning OA (BBOA), more-oxidized OOA (MO-OOA) and less-oxidized OOA (LO-OOA). Adding an additional factor resulted in splitting of COA factor, decreasing it to four factors caused mixing between the MO-OOA and COA factors. Therefore, 5 factor-solution was determined across the whole year. In addition, site-specific factor profiles were derived for HOA, COA, and BBOA through a seasonal bootstrap PMF analysis for winter (Dec, Jan, and Feb) and used as constraints as suggested in Chen et al. (2022) and Via et al. (2022). However, the MY site is surrounded by many restaurants with prevalent cooking emissions. Thus, the chemical fingerprint for both HOA and COA might not be fully separated. Therefore, we constrained the trend of NO<sub>x</sub> time series, BBOA and COA profiles from a previous winter bootstrap solution collected in London North Kensington (2015-2018, Chen et al., 2022) to retrieve environmentally reasonable results with five factors in winter data, so-called base case solution. Then, a bootstrap resampling analysis with 100 iterations and five factors was conducted by constraining the factor profiles of HOA, COA, and BBOA from the base case with random a-value from 0.1-0.5 with step of 0.1. It results in stable factor profiles of these three primary sources as shown in Fig. S2, which shows good agreements with published reference profiles (Chen et al., 2022; Crippa et al., 2013).

Rolling PMF was conducted with a time window of 14 days and a step of 1 day by constraining primary factor profiles of HOA, COA, BBOA in Fig. S2 (averaged bootstrap results) and two additional unconstrained factors with bootstrap resampling and the random a-value option (0.1-0.5, step of 0.1, 50 iterations/window). A criteria list including selections based on both time series and factor profiles as shown in Table S1 was applied as per Chen et al. (2022). With the help of *t*-test in temporal-based criteria (1-3), we can minimize subjective judgements in determining the environmentally reasonable results. Eventually, 3,166 runs (14.1%) of the PMF runs were selected across different rolling windows across the whole year to average as the final results (utilized a-values were averaged to two decimal places) with 4.9 % unmodelled data points, which is comparable with other rolling PMF analyses (Chen et al., 2022).

### 2.5 Meteorological normalisation using boot regression tree model

Meteorological normalisation, also known as deweathering analysis, has been conducted using the "worldmet" R package (Carslaw, 2025) to build boot regression tree (BRT) models for all resolved OA factors from PMF as well as chemical species measured. Considered variables, included relative humidity, wind speed, wind direction, and air temperature trend, hours of the day (local time), day of the week, Julian dates, week of the year as suggested by Carslaw, (2025). While Grange and Carslaw (2019) have also suggested boundary layer height, air mass cluster, or back trajectory information would be beneficial to include to deal with pollutants primarily controlled by regional scale process. However, the aim of this study is understanding how COVID-related policies affect primary/local emission sources (i.e., BC, HOA, COA, and BBOA), which will not be affected significantly regional process, therefore additional metrics will most likely not improve the quantification of these PM components. It is consistent and comparable with previous studies (Font et al., 2022; Grange et al., 2021; Yao and Zhang, 2024) that includes similar meteorological

parameters (i.e., wind speed, wind direction, relative humidity, temperature). In addition, since the trained BRT models are sufficiently good even without considering boundary layer height and back trajectories, performing random forest model will not improve the model significantly, nor change the results drastically as suggested by Yao and Zhang (2024). Thus, in this study, only BRT models were trained and the meteorological effects subsequently removed (i.e., relative humidity, wind speed, wind direction, and air temperature) on all PM/OA.

### 3 Results and Discussions

### 3.1 Model performance of meteorological normalisation

The performance of each model (for individual species/source) is shown in Table S2 with slopes from 0.97 to 1.02 and R<sup>2</sup> (Pearson) from 0.77 to 0.94, which have similar or somewhat better performances compared with previous studies (Font et al., 2022; Grange et al., 2018, 2021; Grange and Carslaw, 2019; Krechmer et al., 2018; Shi et al., 2021; Yao and Zhang, 2024). As shown in the SI (Fig. S8 and Fig. S9) and the lower panel of Figure 5, meteorological effects were generally considerable, especially for Pre-lockdown Spring period, while it does not change the conclusion of the effects from lockdown and EOTHO policies. Therefore, the main results presented in this study are based on the original measurements.

### 3.2 Chemical composition of submicron PM for different periods around the

### COVID-19 Lockdown

The average PM<sub>1</sub> mass concentration at MY site was 11 μg/m<sup>3</sup> for the study period with 44% OA, 21% NO<sub>3</sub>, 15% SO<sub>4</sub>, 16% BC, 5% NH<sub>4</sub>, and 0.6% Cl. The distribution of the chemical composition on PM<sub>1</sub> varied depending on the season and variation was associated with the lockdown and

EOTHO policies (Figure 1). PM<sub>1</sub> increased by 95% in lockdown spring (Mar 26<sup>th</sup>–May 31<sup>st</sup>, 2020) 228 compared to pre-lockdown spring (Mar 1<sup>st</sup>–Mar 25<sup>th</sup>, 2020). Specifically, Org, SO<sub>4</sub>, NO<sub>3</sub>, NH<sub>4</sub>, 229 230 and Cl all increased by 87%, 211%, 73%, 237%, and 132%, respectively. Except for BC, which 231 decreased by 52%. This is due to the polluted airmass originating from mainland Europe and the 232 enhanced agricultural emissions in spring from the UK and wider continental Europe (Aksoyoglu 233 et al., 2020). It was further confirmed, through back trajectory analysis, that elevated PM<sub>1</sub> events (Mar 25<sup>th</sup>–Mar 28<sup>th</sup>, Apr 8<sup>th</sup>–Apr 10<sup>th</sup>, and Apr 15<sup>th</sup>–Apr 17<sup>th</sup>), where the result of airmasses passing 234 235 over northern continental Europe (Fig. S6). In addition, the Org, SO<sub>4</sub>, NO<sub>3</sub>, NH<sub>4</sub>, and Cl were only 236 increased by 21%, 107%, 50%, and 28% respectively after the deweathering analysis (Fig. S8), 237 suggesting significant meteorological influences during this period. NO<sub>3</sub> concentration reduced in 238 summer 2019 and 2020 as expected compared to spring or fall seasons due to the semi-volatile 239 nature of NH<sub>4</sub>NO<sub>3</sub> and lower agricultural emissions, while SO<sub>4</sub> concentrations increased in 240 summer due to enhanced photochemistry across Europe (Bressi et al., 2021; Chen et al., 2022). 241 During the lockdown in spring, SO<sub>4</sub> concentrations remained high, which was associated with 242 long-range transport and marine aerosols (e.g., methanesulfonic acid, MSA) (Fig. S7).

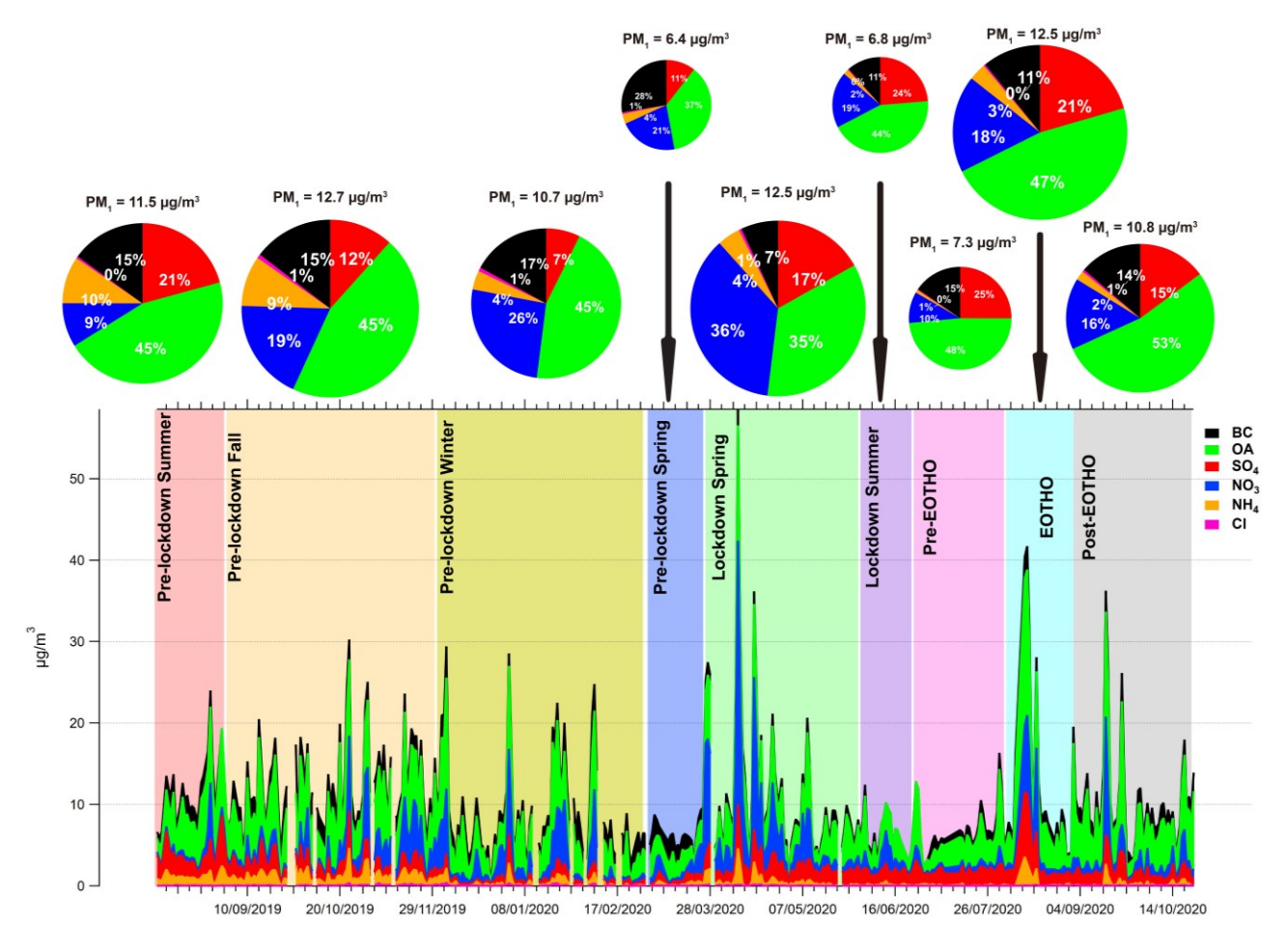


Figure 1 Chemical compositions of PM<sub>1</sub> at MY from Aug 2019 to Oct 2020 (daily resolution) and averaged for the different periods as shown in Table 1.

BC concentrations during the spring lockdown (Mar 26<sup>th</sup>–May 31<sup>st</sup> 2020) reduced from 1.78 to 0.86 μg/m³ (-52%) compared to the pre-lockdown level in spring (Mar 1<sup>st</sup>–Mar 25<sup>th</sup>), due to the significant reduction in traffic during the first lockdown (Transport for London, 2020). Similar decreasing of BC has been observed elsewhere during COVID lockdown as described in introduction (Gamelas et al., 2023; Jeong et al., 2022; Petit et al., 2021; Tian et al., 2021; Xu et al., 2020). It is worth noting that the BC concentration had already reduced by 3% in pre-lockdown spring (Mar 1<sup>st</sup>–Mar 25<sup>th</sup>) compared to the pre-lockdown winter. This is likely due to vehicle mileage reducing as the UK government implemented travel restrictions and advised people to work from home on Mar 16<sup>th</sup>, 2020 (Transport for London, 2020). BC increased to 1.13 μg/m³

(+44%) after the lockdown and before the EOTHO (Jun 24<sup>th</sup>–Aug 2<sup>nd</sup>,2020, pre-EOTHO in Figure 1) as people returned to work and travel. However, BC concentrations remained 34% lower than the pre-lockdown summer (Aug 1<sup>st</sup>–Aug 31<sup>st</sup>, 2019) concentration of 1.72 μg/m³ (Fig. S9), which suggests that the traffic emissions reduced considerably as the fewer economic activities even after the ease of the first lockdown (e.g., suggestions of hybrid working mode, restricted international travel, reduced tourism, limited access to entertainments). BC also increased to 1.35 μg/m³ (+19%) during the EOTHO scheme (Aug 3<sup>rd</sup>–Aug 31<sup>st</sup>, 2020). This was not only because of increased traffic emission during this period, but may also result from cooking activities (e,g, barbecuing or wood-fired cooking styles) in Central London (Defra, 2023). Since the EOTHO was only in place from Mon to Wed, BC concentrations (likely due to increased traffic and cooking emissions) increased on Mon-Wed compared to post-lockdown but before EOTHO (Jun 24<sup>th</sup>–Aug 2<sup>nd</sup>, 2020) (Fig. S10).

### 3.3 OA sources in Central London

As mentioned above, the rolling PMF analysis resolved 5 factor solutions, including HOA, COA, BBOA, MO-OOA, and LO-OOA as shown in Figure 3 and Figure 4. The left panel of Figure 3 shows the yearly averaged factor profiles of resolved PMF factors and total OOA calculated as the sum of LO-OOA and MO-OOA. All factors show good agreements with previous studies in terms of key *m/z* tracers. In addition, as shown in Figure 2, the contribution to total OA concentrations from HOA, BBOA, and LO-OOA was consistent at different OA concentrations. However, the contribution of COA increased as total OA concentrations increased. This suggests that cooking emissions in Central London are responsible for elevated OA concentrations, which was also the case in Athens as shown in Chen et al. (2022).

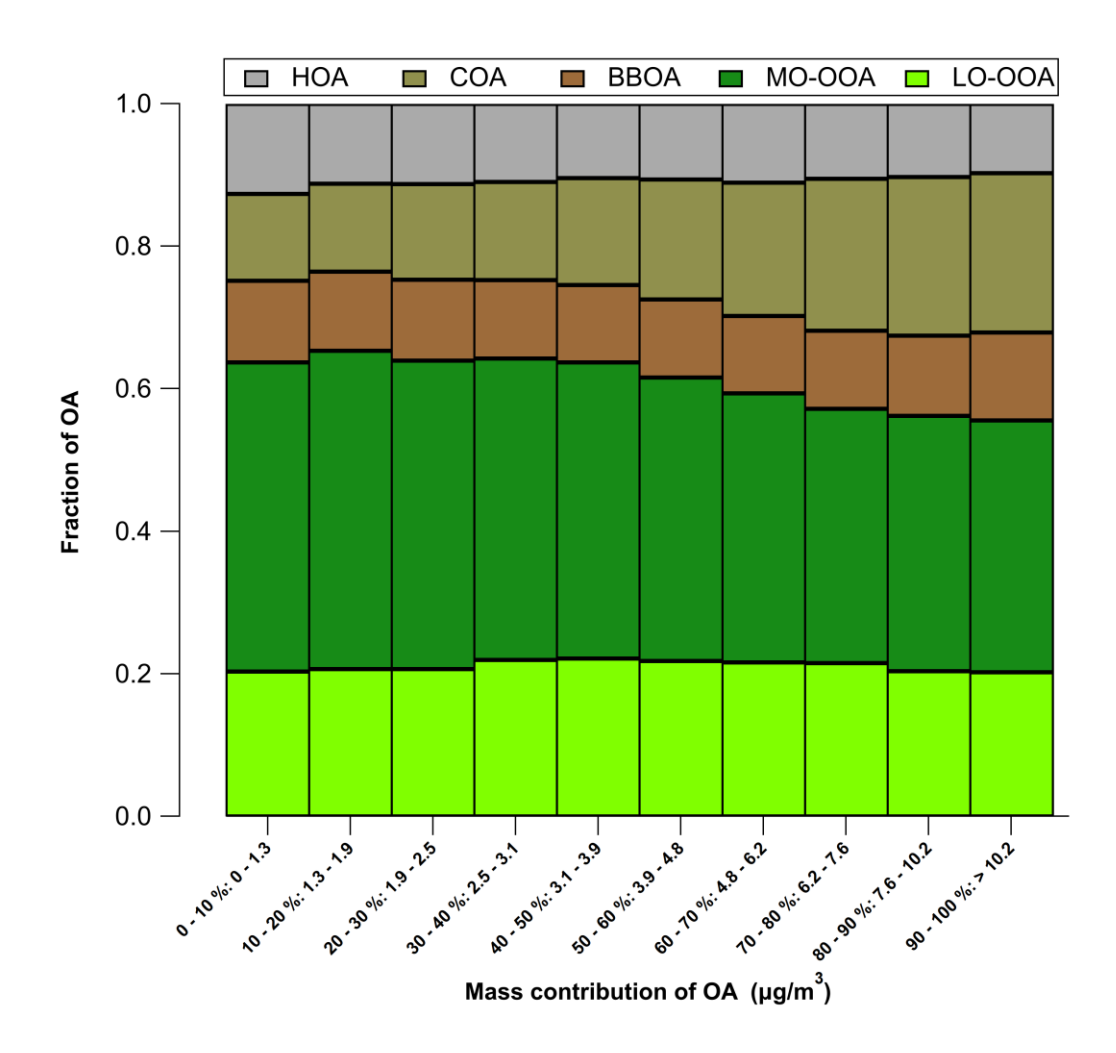


Figure 2 Contributions to total OA from the different identified OA sources at different OA concentrations. Total OA concentrations were split in 10 equally distributed bins.

#### 3.3.1 General characteristics of OA factors

The right panel of Figure 3 shows time series (daily averaged) and Figure 4 shows diurnal cycles for each OA factor. The mean concentrations of HOA, COA, BBOA, MO-OOA, LO-OOA, and OOA (MO-OOA+LO-OOA) were  $0.50 \pm 0.1~\mu g/m^3$ ,  $0.93 \pm 0.14~\mu g/m^3$ ,  $0.55 \pm 0.11~\mu g/m^3$ ,  $1.81 \pm 0.41~\mu g/m^3$ ,  $1.00 \pm 0.44~\mu g/m^3$ , and  $2.80 \pm 0.70~\mu g/m^3$ , and contributed to OA (PM<sub>1</sub>) with the fractions of 11% (5% to PM<sub>1</sub>), 20% (9% to PM<sub>1</sub>), 12% (5% to PM<sub>1</sub>), 38% (17% to PM<sub>1</sub>), 21% (9% to PM<sub>1</sub>), and 59% (26% to PM<sub>1</sub>), respectively. The concentration of all OA factors shows strong time variations over the year as shown on the Figure 4. OA factors also showed seasonality besides

the effects from COVID-related policies (Figure 4 and Fig. S3). POA concentrations were generally lower in the warmer seasons than in winter as lower temperature favours particle formation via condensation and dilution and dispersion are reduced due to the lower boundary layer. It's worth mentioning that the reduced POA concentrations in the warm season was not caused by reduced residential heating and energy consummation since Central London mainly uses natural gas and renewable energy rather than solid fuel combustions (Cliff et al., 2025). The OOA factor concentrations remain relatively consistent across seasons, while its contribution was larger during the warmer seasons (Fig. S4). This is because both high temperature and strong solar radiation will enhance the photochemistry and evaporation of POA sources, and increased volatile organic compound (VOC) emissions lead to high OOA production despite the evaporation of semi-volatile OOA (Fig. S4) (Chen et al., 2022). The temporal variations observed here in Central London was consistent with the other urban sites across Europe (Chen et al., 2022). Therefore, this study focuses on the impacts of COVID-related polices on OA sources.

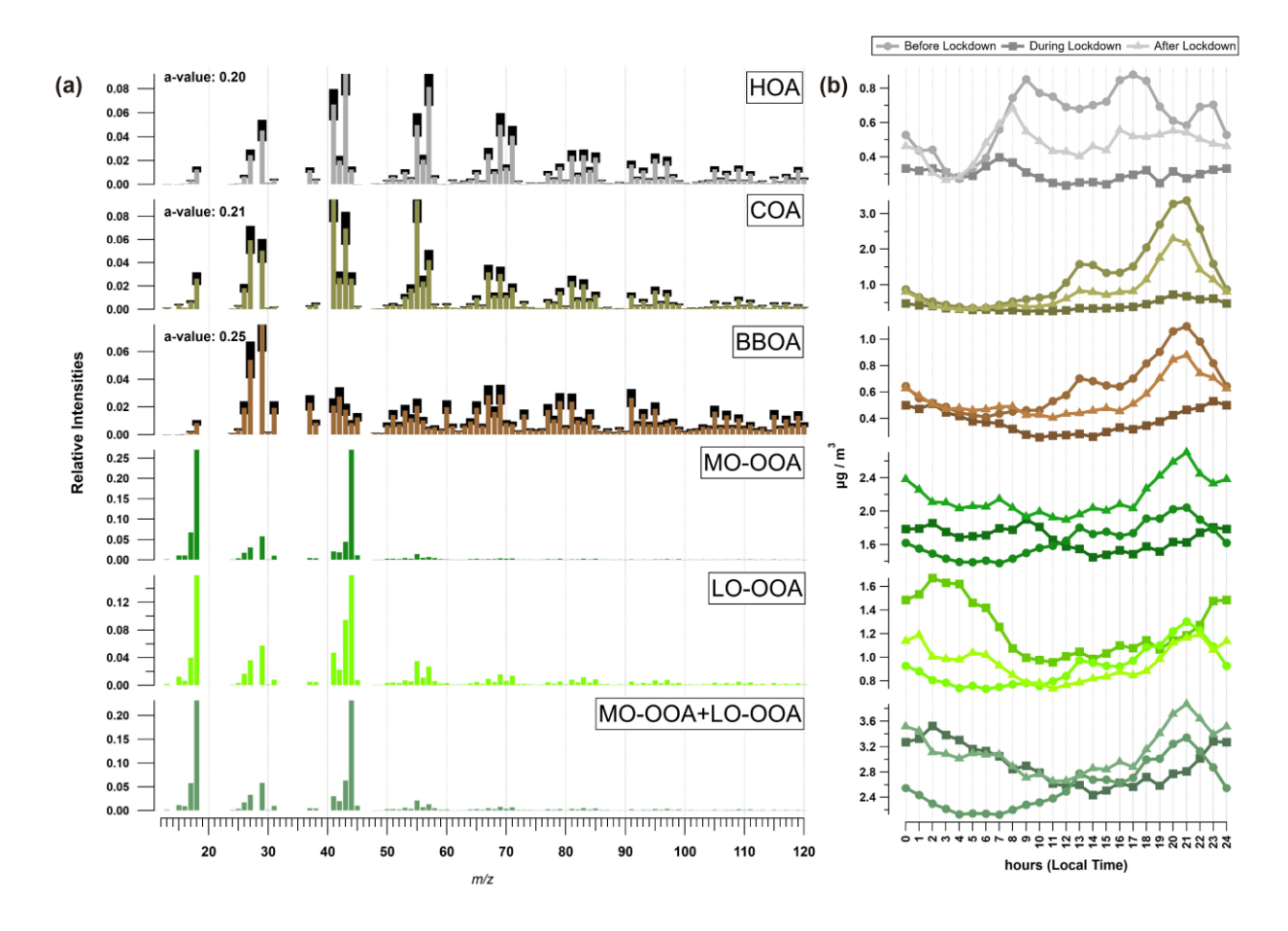


Figure 3 Yearly averaged profiles (a) and diurnal cycles (b) of resolved factors from the rolling PMF analysis at the MY site.

Time is expressed in local time.

The right side of Figure 3 shows the diurnal cycles before, during, and after the lockdown. POA factors showed distinct diurnal variations, in which HOA showed morning and evening rush hour peaks, COA showed distinct lunchtime and evening peaks, and BBOA showed a similar pattern as COA before and after the lockdown. This indicates that the part of what is measured as BBOA in Central London is most likely co-emitted from cooking activity, most likely from barbecuing style or wood-oven pizza restaurants in the area. A survey about use of domestic fuels in the hospitality sector was conducted by Department for Environment Food and Rural Affairs (Defra), UK suggested that restaurants use solid fuel to cook to provide unique flavours (Defra, 2023). Mohr et al. (2009) showed that meat-cooking can slightly elevate m/z 60, which is an important

ion in the BBOA factor profile. OOA factors showed much less diurnal variation compared to POA factors in all periods, this is in agreement with the other 22 European sites reported in Chen et al. (2022). The MO-OOA showed a smaller diurnal variation compared to LO-OOA. This is because the LO-OOA is also known as semi-volatile OOA (SV-OOA), which evaporate during the day due to higher temperatures and accumulate in the evening due to the shallower boundary layer (Chen et al., 2022).

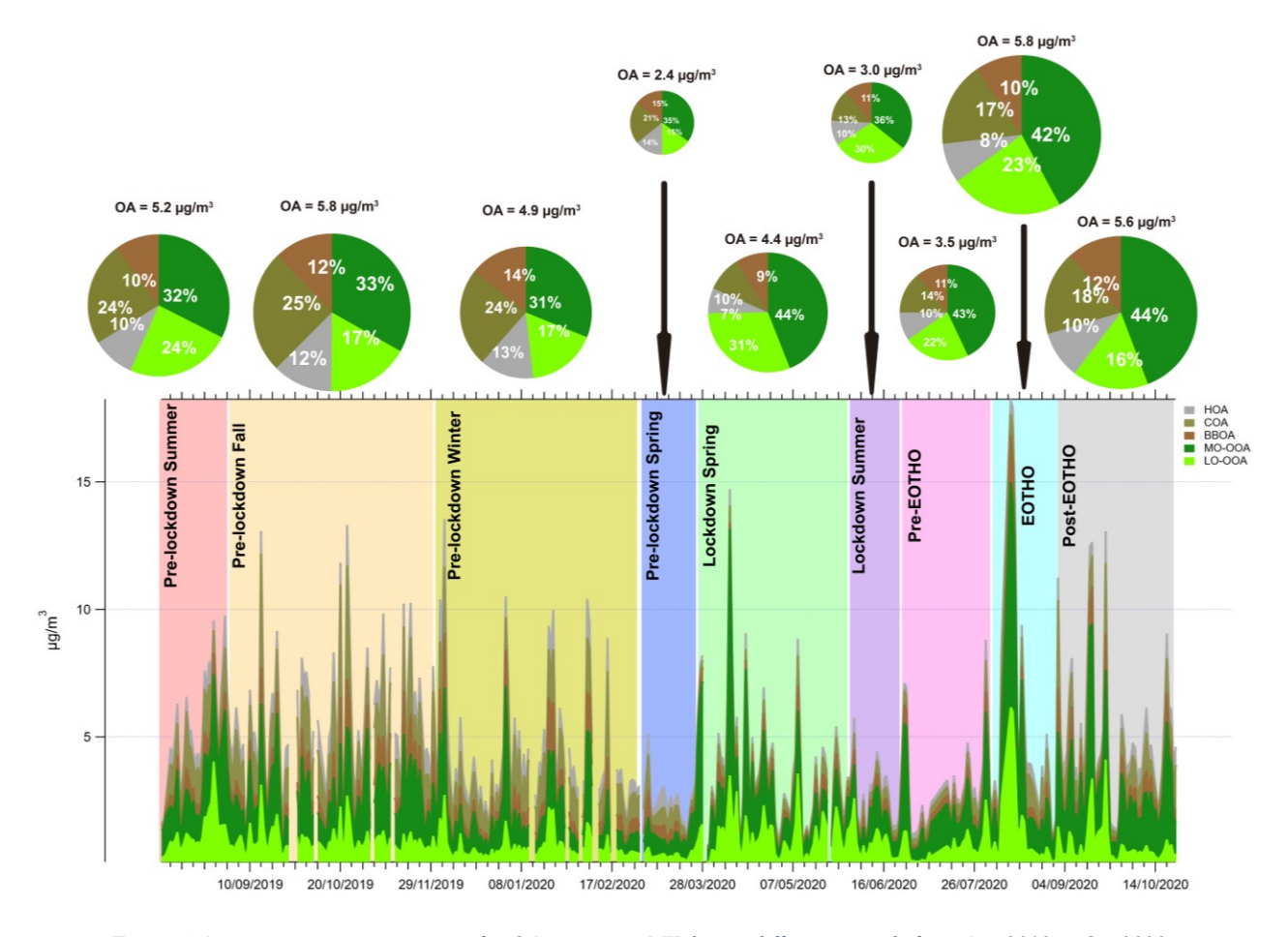


Figure 4 Average mass concentrations for OA sources at MY during different periods from Aug 2019 to Oct 2020

### 3.3.2 Pre-lockdown Spring Pre-lockdown Spring

In general, OA concentration decreased by 51% in pre-lockdown spring compared to pre-lockdown winter (Dec 1<sup>st</sup>, 2019–Feb 28<sup>th</sup>, 2020) due to seasonality, origins of airmass (Fig. S5), and the impact of lockdown. OOA concentrations also decreased drastically by 50%. Primary

emissions were significantly lower due to reduced vehicle mileage and other economic activity before the official lockdown measure came into force on March 26<sup>th</sup> 2020 (Figure 4) as suggested by the 1<sup>st</sup> quarter drop in GDP (ONS, 2022). Atmospheric components related to vehicle emissions (HOA and BC) decreased by 48% and 3% respectively, in early March 2020. COA decreased by 58% due to fewer restaurant activity, BBOA decreased by 50% was likely due to the reduced commercial cooking using charcoal and wood as well as warmer weather requiring less domestic space heating.

#### 3.3.3 Lockdown

326

327

328

329

330

331

332

333

334

335

336

337

338

339

340

341

342

343

344

345

346

347

348

The diurnal variation of COA and BBOA during lockdown showed much less intensity overall but the distinctive lunchtime peak remained as the pre-lockdown; and the evening peak reduced its intensity (Figure 3 b). HOA retained distinct morning and evening rush hour peaks but at lower mass concentrations during lockdown (Figure 3 b). This is because the takeout activities of some restaurants were still active as well as the potential increases for residential cooking activities during lockdown. After the first lockdown, the distinct lunch and evening peaks in diurnal patterns of COA and BBOA reappeared as the open-up of nearby restaurants. The morning and evening rush hour peaks for HOA enhanced considerably as the ease of the travel restrictions after the first lockdown. However, POA concentrations did not reach pre-COVID levels (Figure 5). This is likely due to widespread hybrid working and the remaining oversea travel restrictions supressing tourism, which reduced traffic activity and restaurants visits. Conversely, OOA concentrations during lockdown were slightly higher than pre-lockdown levels. These were related to long-range transport, with relatively high mass concentrations of MO-OOA and LO-OOA during the lockdown (Fig. S5 and Fig. S6). Compared to the pre-lockdown spring, HOA and COA in the lockdown spring decreased by 11% and 15%, respectively, while BBOA increased marginally by

13% (from 0.35 to 0.39 μg/m³) (Figure 5). MO-OOA and LO-OOA increased by 136% and 279%, respectively due to long-range transportation of airmasses from continental Europe (Fig. S5 and Fig. S6) and increased photochemistry (enhanced temperature and ozone levels in Fig. S4) compared to the first 25 days in Mar 2020. This was accompanied by increased SO<sub>4</sub> (+211%), NH<sub>4</sub> (+132%) and NO<sub>3</sub> (+237%) as shown in Fig. S9, despite the higher temperature could favour partitioning these species into the gas phase.

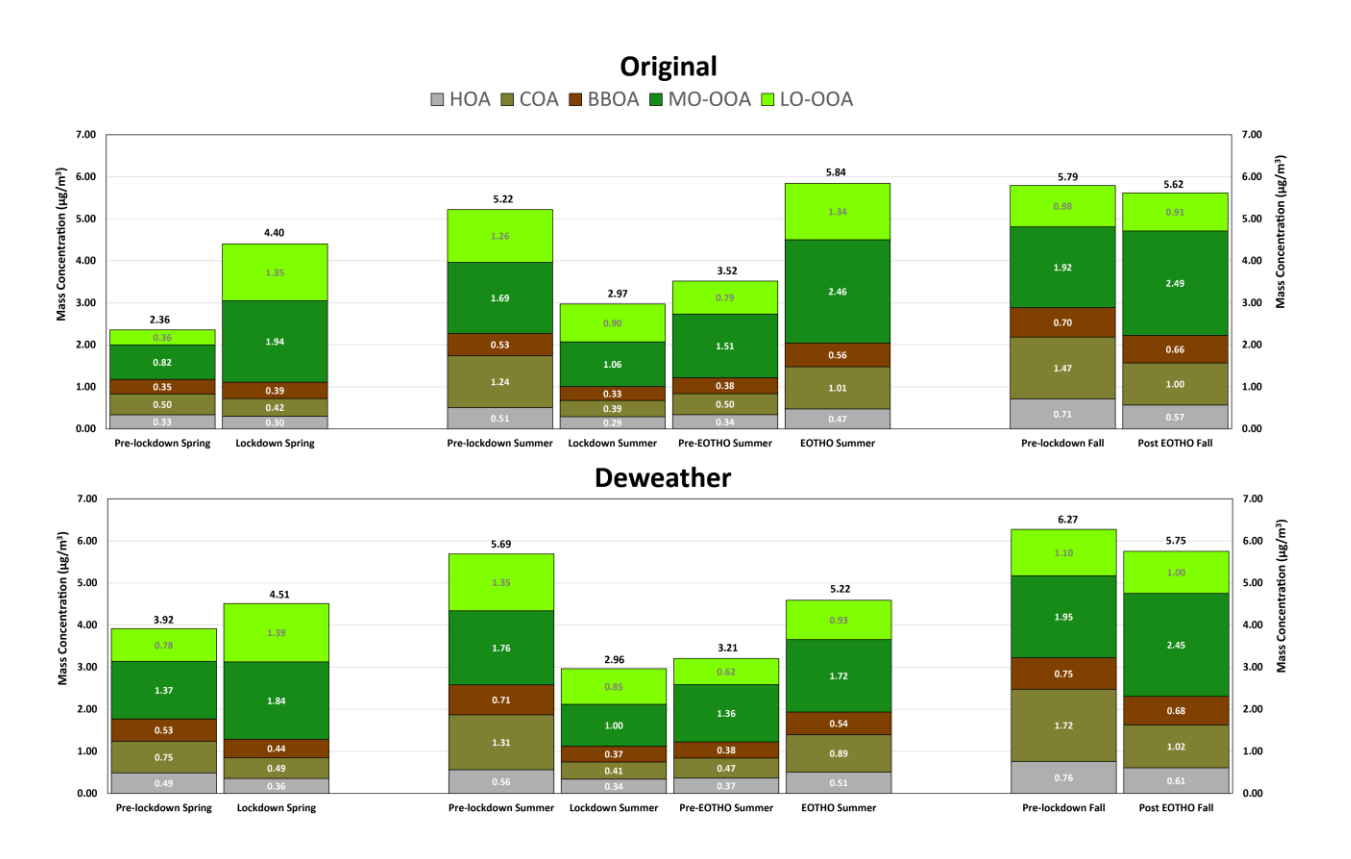


Figure 5 The impacts on OA sources during different periods compared with business-as-usual cases with and without deweathering analysis.

In June 2020, still in lockdown (Jun 1<sup>st</sup>– Jun 23<sup>rd</sup>, 2020), POA showed further but marginal decreases (-3%, -8%, and -15% for HOA, COA, and BBOA, respectively, Figure 4) compared to the lockdown spring as the enhanced photochemistry leads to increased formation of OOA from the POA. However, the overall mass concentration of MO-OOA and LO-OOA decreased

363 significantly by 45%, and 34%, respectively as the result of fewer long-range transported airmasses

364 (Fig. S5).

#### 3.3.4 Pre-EOTHO

During pre-EOTHO (Jun 24<sup>th</sup>–Aug 2<sup>nd</sup>, 2020) after the lockdown policy was eased, HOA, COA, and BBOA all showed considerably increases of 16%, 30%, and 14%, respectively when compared to lockdown summer period. In which, MO-OOA increased by 45% and LO-OOA decreased by 13%, respectively as the relatively higher temperature and solar radiation favoured the evaporation of LO-OOA and production of MO-OOA from LO-OOA and POA. As shown in Figure 5, the POA concentrations were much lower when compared to summer 2019 (Aug 1<sup>st</sup>–Aug 31<sup>st</sup>, 2019) as travel and economic activities did not return to pre-COVID levels (ONS, 2022; Transport for London, 2020). Specifically, lower HOA (-33%), BC (-37%) due to reduced vehicle mileage resulted, and COA (-59%) due to the reduced commercial cooking activity. As BBOA is coemitted with COA during of cooking activities, BBOA also decreased slightly from 0.53 to 0.38 μg/m³ (-28%, Figure 5).

### 3.3.5 Eat Out To Help Out (EOTHO)

EOTHO policy (Aug 3<sup>rd</sup>–Aug 31<sup>st</sup>, 2020) had a significant impact on all POA factors. In particular, the COA concentration increased by 100% compared to the post-lockdown period (Pre-EOTHO Summer) from Jun 24<sup>th</sup> to Aug 2<sup>rd</sup>, 2020 (0.5 to 1.0 μg/m³, Figure 6). HOA and BBOA concentrations also increased by 40% and 48%, respectively, which suggested the human activities resulting in these emissions recovered slowly after the lockdown (ONS, 2022; Transport for London, 2020). COA was significantly higher due to EOTHO, however, it did not reach pre-

COVID concentrations (Figure 5 and Figure 6) as its level was lower on each weekday except for Mon.

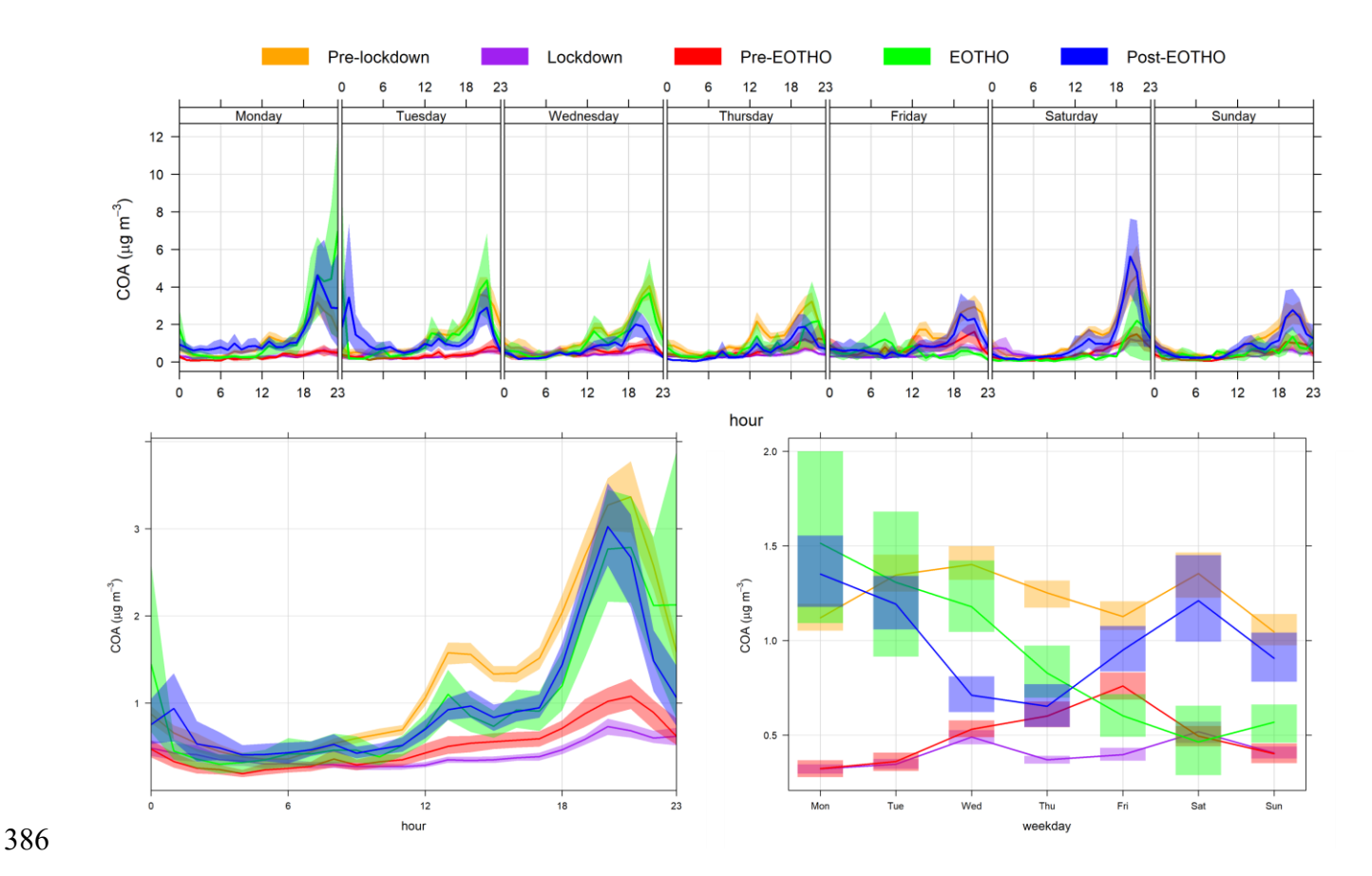


Figure 6 . COA diurnal plots for each weekday, diurnal plots, and weekly plots at different periods in relation with COVIDrelated policies

EOTHO only operated from Mon to Wed, and this was clear in the diurnal plots (Figure 6 and Fig. S12) with larger COA concentrations from Mon to Wed, in contrast with larger concentrations over the weekend (Fri to Sun) before EOTHO (Jun 24<sup>th</sup>–Aug 2<sup>nd</sup>, 2020). Interestingly, even after the EOTHO policy ceased (Sep 1<sup>st</sup>–Oct 22<sup>nd</sup>, 2020), COA levels remained elevated on Mon and Tue but a much higher level during the weekend was observed. This suggests that EOTHO had an influence on the consumer behaviour even after the lockdown. It is also worth noting that the high concentrations of COA and BBOA (Figure 6 and Fig. S11) on Monday night were caused by the last day of EOTHO policy coinciding with a UK public holiday on Aug 31<sup>st</sup>.

Also, during EOTHO, MO-OOA and LO-OOA increased by 63% and 70% respectively compared to post-lockdown concentrations before EOTHO and correlated with increased NH<sub>4</sub>, NO<sub>3</sub> and SO<sub>4</sub> concentrations. This was mainly due to long-ranged transported airmasses (Fig. S5) and enhanced photochemistry with increased temperature and mass concentration of POAs (Fig. S4).

### 4 Conclusion

397

398

399

400

401

402

403

404

405

406

407

408

409

410

411

412

413

414

415

416

417

418

This study demonstrates the importance of source apportionment studies to better understand how national and local government policies can impact the PM mixture, and how these effects can be differentiated from the influences of meteorology and large-scale atmospheric processes. PM concentrations increased at the beginning of the lockdown (Mar-Apr 2020) despite reduced economic activities, which was caused by long-range transported airmasses instead of primary emissions. Through examining the source apportionment (and inorganic PM composition), COVID-related policies were found to have profound but largely unintended impacts on air quality. The first lockdown significantly reduced POA sources: including HOA by 52%, COA by 67%, and BBOA by 42%. While all these components reduced dramatically during the lockdown, they only gradually increased again and did not reach pre-COVID levels during the duration of this study (Aug 2019-Oct 2020). Most significantly, while the Eat Out To Help Out (EOTHO) policy was effective in helping the hospitality industry to recover from economic losses during the lockdown, it had unintended impacts on air quality as cooking emissions increased. Clearly detecting this change confirms the presence of COA (20% to OA) as an important source of OA in London and the importance of commercial cooking as a source. Also of note was the impact that EOTHO had on BBOA concentrations, which increased by 48% while this policy was in place. This establishes a clear

link between commercial cooking activity and BBOA measured in cities due to the use of charcoal and wood as cooking fuels (Defra, 2023), as well as potentially emissions from cooking ingredients. Cooking may therefore be underestimated as a source if COA concentrations are considered in isolation, and BBOA is only associated with other sources of solid fuel burning. This emphasises the need to develop policies and technical solutions to mitigate commercial cooking emissions in the urban environment, especially as there are limited regulations on this industry in terms of air pollution. There are filter technologies (e.g., electrostatic precipitators, UV-C lamp exhaust hood, hydrovents) available that have been implemented as law in Hong Kong to effectively control cooking emissions (Hong Kong EPD, 2024). It also demonstrated the importance in continuous monitoring with subsequent source apportionment analysis to better understand the influence of government policies to improve air quality more effectively.

# Code/Data availability

431

436

444

445

446

447

448

449

450

Rolling PMF analyses is run using SoFi Pro from Datalystica (https://datalystica.com/sofi-pro/,
Datalystica, 2024) under Igor Pro 9 platform from WaveMetrics® (https://www.wavemetrics.com/,
WaveMetrics, 2024) and they are both available for purchase. Raw data/results from the study are
available upon request to the corresponding author Gang I. Chen (gang.chen@imperial.ac.uk).

### Author contribution

Gang I. Chen: Writing – review & editing, Writing – original draft, Visualization, Validation,
Project administration, Methodology, Investigation, Funding acquisition, Formal analysis, Data
curation, Conceptualization. Anja H. Tremper: Writing – review & editing, Methodology,
Formal analysis, Data curation. Max Priestman: Methodology, Formal analysis, Data curation.
Anna Font: Writing – review & editing, Methodology, Formal analysis, Data curation. David C.
Green: Writing – review & editing, Supervision, Project administration, Methodology, Resources,
Funding acquisition, Conceptualization.

# Competing interests

The authors declare that they have no known competing financial interests or personal relationships that could have appeared to influence the work reported in this paper.

# Acknowledgement

This study is part funded by the National Institute for Health Research (NIHR) Health Protection Research Unit in Environmental Exposures and Health, a partnership between UK Health Security Agency (UKHSA) and Imperial College London. The views expressed are those of the authors and not necessarily those of the NIHR, UKHSA or the Department of Health and Social Care. This study was also supported by NERC Awards (NE/1007806/1)

# References

454

455 Aksoyoglu, S., Jiang, J., Ciarelli, G., Baltensperger, U., and Prévôt, A. S. H.: Role of ammonia 456 in European air quality with changing land and ship emissions between 1990 and 2030, 457 Atmos Chem Phys, 20, 15665–15680, https://doi.org/10.5194/acp-20-15665-2020, 458 2020. 459 Allan, J. D., Delia, A. E., Coe, H., Bower, K. N., Alfarra, M. R., Jimenez, J. L., Middlebrook, 460 A. M., Drewnick, F., Onasch, T. B., Canagaratna, M. R., Jayne, J. T., and Worsnop, D. 461 R.: A generalised method for the extraction of chemically resolved mass spectra from 462 Aerodyne aerosol mass spectrometer data, J Aerosol Sci, 35, 909–922, 463 https://doi.org/10.1016/j.jaerosci.2004.02.007, 2004. 464 Bressi, M., Cavalli, F., Putaud, J. P., Fröhlich, R., Petit, J. E., Aas, W., Äijälä, M., Alastuey, A., 465 Allan, J. D., Aurela, M., Berico, M., Bougiatioti, A., Bukowiecki, N., Canonaco, F., 466 Crenn, V., Dusanter, S., Ehn, M., Elsasser, M., Flentje, H., Graf, P., Green, D. C., 467 Heikkinen, L., Hermann, H., Holzinger, R., Hueglin, C., Keernik, H., Kiendler-Scharr, 468 A., Kubelová, L., Lunder, C., Maasikmets, M., Makeš, O., Malaguti, A., Mihalopoulos, 469 N., Nicolas, J. B., O'Dowd, C., Ovadnevaite, J., Petralia, E., Poulain, L., Priestman, M., 470 Riffault, V., Ripoll, A., Schlag, P., Schwarz, J., Sciare, J., Slowik, J., Sosedova, Y., 471 Stavroulas, I., Teinemaa, E., Via, M., Vodička, P., Williams, P. I., Wiedensohler, A., 472 Young, D. E., Zhang, S., Favez, O., Minguillón, M. C., and Prevot, A. S. H.: A European

473	aerosol phenomenology - 7: High-time resolution chemical characteristics of submicron
474	particulate matter across Europe, Atmos Environ X, 10, 100108,
475	https://doi.org/10.1016/J.AEAOA.2021.100108, 2021.
476	Canonaco, F., Tobler, A., Chen, G., Sosedova, Y., Slowik, J. G., Bozzetti, C., Daellenbach, K.
477	R., El Haddad, I., Crippa, M., Huang, RJ., Furger, M., Baltensperger, U., and Prévôt,
478	A. S. H.: A new method for long-term source apportionment with time-dependent factor
479	profiles and uncertainty assessment using SoFi Pro: application to 1 year of organic
480	aerosol data, Atmos Meas Tech, 14, 923-943, https://doi.org/10.5194/amt-14-923-2021,
481	2021.
482	Carslaw, D.: deweather: Remove the influence of weather on air quality data, https://openair-
483	project.github.io/deweather/, 2025.
484	Chebaicheb, H., de Brito, J. F., Amodeo, T., Couvidat, F., Petit, JE., Tison, E., Abbou, G.,
485	Baudic, A., Chatain, M., Chazeau, B., Marchand, N., Falhun, R., Francony, F., Ratier,
486	C., Grenier, D., Vidaud, R., Zhang, S., Gille, G., Meunier, L., Marchand, C., Riffault,
487	V., and Favez, O.: Multiyear high-temporal-resolution measurements of submicron
488	aerosols at 13 French urban sites: data processing and chemical composition, Earth Syst
489	Sci Data, 16, 5089-5109, https://doi.org/10.5194/essd-16-5089-2024, 2024.
490	Chen, G., Canonaco, F., Tobler, A., Aas, W., Alastuey, A., Allan, J., Atabakhsh, S., Aurela, M.,
491	Baltensperger, U., Bougiatioti, A., De Brito, J. F., Ceburnis, D., Chazeau, B.,
492	Chebaicheb, H., Daellenbach, K. R., Ehn, M., El Haddad, I., Eleftheriadis, K., Favez,
493	O., Flentje, H., Font, A., Fossum, K., Freney, E., Gini, M., Green, D. C., Heikkinen, L.,
494	Herrmann, H., Kalogridis, AC., Keernik, H., Lhotka, R., Lin, C., Lunder, C.,
495	Maasikmets, M., Manousakas, M. I., Marchand, N., Marin, C., Marmureanu, L.,

496 Mihalopoulos, N., Močnik, G., Necki, J., O'Dowd, C., Ovadnevaite, J., Peter, T., Petit, 497 J.-E., Pikridas, M., Matthew Platt, S., Pokorná, P., Poulain, L., Priestman, M., Riffault, 498 V., Rinaldi, M., Różański, K., Schwarz, J., Sciare, J., Simon, L., Skiba, A., Slowik, J. 499 G., Sosedova, Y., Stavroulas, I., Styszko, K., Teinemaa, E., Timonen, H., Tremper, A., 500 Vasilescu, J., Via, M., Vodička, P., Wiedensohler, A., Zografou, O., Cruz Minguillón, 501 M., and Prévôt, A. S. H.: European aerosol phenomenology – 8: Harmonised source 502 apportionment of organic aerosol using 22 Year-long ACSM/AMS datasets, Environ 503 Int, 166, 107325, https://doi.org/10.1016/j.envint.2022.107325, 2022. 504 Cliff, S. J., Drysdale, W., Lewis, A. C., Møller, S. J., Helfter, C., Metzger, S., Liddard, R., 505 Nemitz, E., Barlow, J. F., and Lee, J. D.: Evidence of Heating-Dominated Urban NOx 506 Emissions, Environ Sci Technol, 59, 4399-4408, 507 https://doi.org/10.1021/acs.est.4c13276, 2025. 508 Crippa, M., DeCarlo, P. F., Slowik, J. G., Mohr, C., Heringa, M. F., Chirico, R., Poulain, L., 509 Freutel, F., Sciare, J., Cozic, J., Di Marco, C. F., Elsasser, M., Nicolas, J. B., Marchand, 510 N., Abidi, E., Wiedensohler, A., Drewnick, F., Schneider, J., Borrmann, S., Nemitz, E., 511 Zimmermann, R., Jaffrezo, J.-L., Prévôt, A. S. H., and Baltensperger, U.: Wintertime 512 aerosol chemical composition and source apportionment of the organic fraction in the 513 Paris, metropolitan of Chem Phys, 13, 961–981, area Atmos 514 https://doi.org/10.5194/acp-13-961-2013, 2013. 515 Defra: Use of domestic fuels in the hospitality sector – a qualitative review of hospitality 516 businesses, 2023. 517 Dominici, F., Peng, R. D., Bell, M. L., Pham, L., McDermott, A., Zeger, S. L., and Samet, J. 518 M.: Fine Particulate Air Pollution and Hospital Admission for Cardiovascular and

519	Respiratory Diseases, JAMA, 295, 1127, https://doi.org/10.1001/jama.295.10.1127,
520	2006.
521	European Environment Agency: Europe's air quality status 2024, https://doi.org/10.2800/5970,
522	2024.
523	European Union: Directive (EU) 2024/2881 of the European Parliament and of the Council of
524	23 October 2024 on ambient air quality and cleaner air for Europe (recast), 2024.
525	Font, A., Ciupek, K., Butterfield, D., and Fuller, G. W.: Long-term trends in particulate matter
526	from wood burning in the United Kingdom: Dependence on weather and social factors,
527	Environmental Pollution, 314, 120105, https://doi.org/10.1016/j.envpol.2022.120105,
528	2022.
529	Fröhlich, R., Cubison, M. J., Slowik, J. G., Bukowiecki, N., Prévôt, A. S. H., Baltensperger, U.,
530	Schneider, J., Kimmel, J. R., Gonin, M., Rohner, U., Worsnop, D. R., and Jayne, J. T.:
531	The ToF-ACSM: a portable aerosol chemical speciation monitor with TOFMS detection
532	Atmos Meas Tech, 6, 3225–3241, https://doi.org/10.5194/amt-6-3225-2013, 2013.
533	Gamelas, C. A., Canha, N., Vicente, A., Silva, A., Borges, S., Alves, C., Kertesz, Z., and
534	Almeida, S. M.: Source apportionment of PM2.5 before and after COVID-19 lockdown
535	in an urban-industrial area of the Lisbon metropolitan area, Portugal, Urban Clim, 49,
536	101446, https://doi.org/10.1016/j.uclim.2023.101446, 2023.
537	Grange, S. K. and Carslaw, D. C.: Using meteorological normalisation to detect interventions
538	in air quality time series, Science of The Total Environment, 653, 578-588,
539	https://doi.org/10.1016/j.scitotenv.2018.10.344, 2019.

540 Grange, S. K., Carslaw, D. C., Lewis, A. C., Boleti, E., and Hueglin, C.: Random forest 541 meteorological normalisation models for Swiss PM <sub>10</sub> trend analysis, Atmos Chem Phys, 542 18, 6223–6239, https://doi.org/10.5194/acp-18-6223-2018, 2018. 543 Grange, S. K., Lee, J. D., Drysdale, W. S., Lewis, A. C., Hueglin, C., Emmenegger, L., and 544 Carslaw, D. C.: COVID-19 lockdowns highlight a risk of increasing ozone pollution in 545 European urban areas, Atmos Chem Phys, 21, 4169–4185, https://doi.org/10.5194/acp-546 21-4169-2021, 2021. 547 Hass-Mitchell, T., Joo, T., Rogers, M., Nault, B. A., Soong, C., Tran, M., Seo, M., Machesky, 548 J. E., Canagaratna, M., Roscioli, J., Claflin, M. S., Lerner, B. M., Blomdahl, D. C., 549 Misztal, P. K., Ng, N. L., Dillner, A. M., Bahreini, R., Russell, A., Krechmer, J. E., 550 Lambe, A., and Gentner, D. R.: Increasing Contributions of Temperature-Dependent 551 Oxygenated Organic Aerosol to Summertime Particulate Matter in New York City, ACS 552 ES&T Air, 1, 113–128, https://doi.org/10.1021/acsestair.3c00037, 2024. 553 Hong Kong EPD: Control of Oily Fume and Cooking Odour from Restaurants and Food 554 Business, 2024. 555 Hu, R., Wang, S., Zheng, H., Zhao, B., Liang, C., Chang, X., Jiang, Y., Yin, R., Jiang, J., and 556 Hao, J.: Variations and Sources of Organic Aerosol in Winter Beijing under Markedly 557 Reduced Anthropogenic Activities During COVID-2019, Environ Sci Technol, 56, 558 6956–6967, https://doi.org/10.1021/acs.est.1c05125, 2022. 559 IPCC: Climate Change 2021 – The Physical Science Basis, Cambridge University Press, 560 https://doi.org/10.1017/9781009157896, 2021. 561 Jayne, J. T., Leard, D. C., Zhang, X., Davidovits, P., Smith, K. A., Kolb, C. E., and Worsnop,

D. R.: Development of an Aerosol Mass Spectrometer for Size and Composition

563 Analysis of Submicron Particles, Aerosol Science and Technology, 33, 49-70, 564 https://doi.org/10.1080/027868200410840, 2000. 565 Jeong, C.-H., Yousif, M., and Evans, G. J.: Impact of the COVID-19 lockdown on the chemical 566 composition and sources of urban PM2.5, Environmental Pollution, 292, 118417, 567 https://doi.org/10.1016/j.envpol.2021.118417, 2022. 568 Jimenez, J. L., Canagaratna, M. R., Donahue, N. M., Prevot, A. S. H. H., Zhang, Q., Kroll, J. 569 H., DeCarlo, P. F., Allan, J. D., Coe, H., Ng, N. L., Aiken, A. C., Docherty, K. S., Ulbrich, I. M., Grieshop, A. P., Robinson, A. L., Duplissy, J., Smith, J. D., Wilson, K. 570 571 R., Lanz, V. A., Hueglin, C., Sun, Y. L., Tian, J., Laaksonen, A., Raatikainen, T., 572 Rautiainen, J., Vaattovaara, P., Ehn, M., Kulmala, M., Tomlinson, J. M., Collins, D. R., 573 Cubison, M. J., Dunlea, J., Huffman, J. A., Onasch, T. B., Alfarra, M. R., Williams, P. 574 I., Bower, K., Kondo, Y., Schneider, J., Drewnick, F., Borrmann, S., Weimer, S., Demerjian, K., Salcedo, D., Cottrell, L., Griffin, R., Takami, A., Miyoshi, T., 575 Hatakeyama, S., Shimono, A., Sun, J. Y., Zhang, Y. M., Dzepina, K., Kimmel, J. R., 576 577 Sueper, D., Jayne, J. T., Herndon, S. C., Trimborn, A. M., Williams, L. R., Wood, E. C., 578 Middlebrook, A. M., Kolb, C. E., Baltensperger, U., Worsnop, D. R., Dunlea, E. J., 579 Huffman, J. A., Onasch, T. B., Alfarra, M. R., Williams, P. I., Bower, K., Kondo, Y., 580 Schneider, J., Drewnick, F., Borrmann, S., Weimer, S., Demerjian, K., Salcedo, D., 581 Cottrell, L., Griffin, R., Takami, A., Miyoshi, T., Hatakeyama, S., Shimono, A., Sun, J. 582 Y., Zhang, Y. M., Dzepina, K., Kimmel, J. R., Sueper, D., Jayne, J. T., Herndon, S. C., Trimborn, A. M., Williams, L. R., Wood, E. C., Middlebrook, A. M., Kolb, C. E., 583 Baltensperger, U., and Worsnop, D. R.: Evolution of Organic Aerosols in the 584

585 Atmosphere, Science (1979), 326, 1525–1529, https://doi.org/10.1126/science.1180353, 586 2009. 587 Joo, T., Rogers, M. J., Soong, C., Hass-Mitchell, T., Heo, S., Bell, M. L., Ng, N. L., and Gentner, 588 D. R.: Aged and Obscured Wildfire Smoke Associated with Downwind Health Risks, 589 Environ Sci Technol Lett, 11, 1340–1347, https://doi.org/10.1021/acs.estlett.4c00785, 590 2024. 591 Kelly, F. J. and Fussell, J. C.: Size, source and chemical composition as determinants of toxicity 592 attributable to ambient particulate matter, Atmos Environ, 60. 504–526, 593 https://doi.org/10.1016/j.atmosenv.2012.06.039, 2012. 594 Krechmer, J., Lopez-Hilfiker, F., Koss, A., Hutterli, M., Stoermer, C., Deming, B., Kimmel, J., 595 Warneke, C., Holzinger, R., Jayne, J., Worsnop, D., Fuhrer, K., Gonin, M., and de Gouw, 596 J.: Evaluation of a New Reagent-Ion Source and Focusing Ion-Molecule Reactor for 597 Use in Proton-Transfer-Reaction Mass Spectrometry, Anal Chem, 90, 12011–12018, 598 https://doi.org/10.1021/acs.analchem.8b02641, 2018. 599 Laj, P., Lund Myhre, C., Riffault, V., Amiridis, V., Fuchs, H., Eleftheriadis, K., Petäjä, T., 600 Salameh, T., Kivekäs, N., Juurola, E., Saponaro, G., Philippin, S., Cornacchia, C., 601 Alados Arboledas, L., Baars, H., Claude, A., De Mazière, M., Dils, B., Dufresne, M., 602 Evangeliou, N., Favez, O., Fiebig, M., Haeffelin, M., Herrmann, H., Höhler, K., Illmann, 603 N., Kreuter, A., Ludewig, E., Marinou, E., Möhler, O., Mona, L., Eder Murberg, L., 604 Nicolae, D., Novelli, A., O'Connor, E., Ohneiser, K., Petracca Altieri, R. M., Picquet-605 Varrault, B., van Pinxteren, D., Pospichal, B., Putaud, J.-P., Reimann, S., Siomos, N., 606 Stachlewska, I., Tillmann, R., Voudouri, K. A., Wandinger, U., Wiedensohler, A., 607 Apituley, A., Comerón, A., Gysel-Beer, M., Mihalopoulos, N., Nikolova, N., Pietruczuk,

608	A., Sauvage, S., Sciare, J., Skov, H., Svendby, T., Swietlicki, E., Tonev, D., Vaughan,
609	G., Zdimal, V., Baltensperger, U., Doussin, JF., Kulmala, M., Pappalardo, G., Sorvari
610	Sundet, S., and Vana, M.: Aerosol, Clouds and Trace Gases Research Infrastructure
611	(ACTRIS): The European Research Infrastructure Supporting Atmospheric Science,
612	Bull Am Meteorol Soc, 105, E1098-E1136, https://doi.org/10.1175/BAMS-D-23-
613	0064.1, 2024.
614	Lippmann, M., Chen, L. C., Gordon, T., Ito, K., and Thurston, G. D.: National Particle
615	Component Toxicity (NPACT) Initiative: Integrated Epidemiologic and Toxicologic
616	Studies of the Health Effects of Particulate Matter Components, Boston, 2013.
617	Liu, F., Joo, T., Ditto, J. C., Saavedra, M. G., Takeuchi, M., Boris, A. J., Yang, Y., Weber, R.
618	J., Dillner, A. M., Gentner, D. R., and Ng, N. L.: Oxidized and Unsaturated: Key
619	Organic Aerosol Traits Associated with Cellular Reactive Oxygen Species Production
620	in the Southeastern United States, Environ Sci Technol, 57, 14150-14161,
621	https://doi.org/10.1021/acs.est.3c03641, 2023.
622	Mebrahtu, T. F., McEachan, R. R. C., Yang, T. C., Crossley, K., Rashid, R., Hossain, R., Vaja,
623	I., and Bryant, M.: Differences in public's perception of air quality and acceptability of
624	a clean air zone: A mixed-methods cross sectional study, J Transp Health, 31, 101654,
625	https://doi.org/10.1016/J.JTH.2023.101654, 2023.
626	Middlebrook, A. M., Bahreini, R., Jimenez, J. L., and Canagaratna, M. R.: Evaluation of
627	Composition-Dependent Collection Efficiencies for the Aerodyne Aerosol Mass
628	Spectrometer using Field Data, Aerosol Science and Technology, 46, 258-271,
629	https://doi.org/10.1080/02786826.2011.620041, 2012.

630 Mohr, C., Huffman, J. A., Cubison, M. J., Aiken, A. C., Docherty, K. S., Kimmel, J. R., Ulbrich, 631 I. M., Hannigan, M., and Jimenez, J. L.: Characterization of primary organic aerosol 632 emissions from meat cooking, trash burning, and motor vehicles with high-resolution 633 aerosol mass spectrometry and comparison with ambient and chamber observations, 634 Environ Sci Technol, 43. 2443-2449. 635 https://doi.org/10.1021/ES8011518/SUPPL FILE/ES8011518 SI 001.PDF, 2009. 636 Mudway, I. S., Dundas, I., Wood, H. E., Marlin, N., Jamaludin, J. B., Bremner, S. A., Cross, 637 L., Grieve, A., Nanzer, A., Barratt, B. M., Beevers, S., Dajnak, D., Fuller, G. W., Font, 638 A., Colligan, G., Sheikh, A., Walton, R., Grigg, J., Kelly, F. J., Lee, T. H., and Griffiths, 639 C. J.: Impact of London's low emission zone on air quality and children's respiratory 640 health: a sequential annual cross-sectional study, Lancet Public Health, 4, e28–e40, 641 https://doi.org/10.1016/S2468-2667(18)30202-0, 2019. 642 Ng, N. L., Herndon, S. C., Trimborn, A., Canagaratna, M. R., Croteau, P. L., Onasch, T. B., 643 Sueper, D., Worsnop, D. R., Zhang, Q., Sun, Y. L., and Jayne, J. T.: An Aerosol 644 Chemical Speciation Monitor (ACSM) for Routine Monitoring of the Composition and 645 Mass Concentrations of Ambient Aerosol, Aerosol Science and Technology, 45, 780– 646 794, https://doi.org/10.1080/02786826.2011.560211, 2011. 647 Oltra, C., Sala, R., López-asensio, S., Germán, S., and Boso, A.: Individual-Level Determinants 648 of the Public Acceptance of Policy Measures to Improve Urban Air Quality: The Case 649 of the Barcelona Low Emission Zone, Sustainability 2021, Vol. 13, Page 1168, 13, 1168, 650 https://doi.org/10.3390/SU13031168, 2021. 651 ONS: GDP and events in history: how the COVID-19 pandemic shocked the UK economy, 652 2022.

653 Petit, J.-E., Dupont, J.-C., Favez, O., Gros, V., Zhang, Y., Sciare, J., Simon, L., Truong, F., 654 Bonnaire, N., Amodeo, T., Vautard, R., and Haeffelin, M.: Response of atmospheric 655 composition to COVID-19 lockdown measures during spring in the Paris region 656 (France), Atmos Chem Phys, 21, 17167–17183, https://doi.org/10.5194/acp-21-17167-657 2021, 2021. Pinakidou, S.: People's perceptions of air pollution and their awareness of official indexes at 658 659 the start of the twenty-first century: a review, Discover Environment 2025 3:1, 3, 1–20, 660 https://doi.org/10.1007/S44274-025-00213-X, 2025. 661 Pye, H. O. T., Ward-Caviness, C. K., Murphy, B. N., Appel, K. W., and Seltzer, K. M.: 662 Secondary organic aerosol association with cardiorespiratory disease mortality in the United States, Nat Commun, 12, 7215, https://doi.org/10.1038/s41467-021-27484-1, 663 664 2021. 665 Seinfeld, J. H., Wiley, J., and Pandis, S. N.: ATMOSPHERIC From Air Pollution to Climate 666 Change SECOND EDITION, 628-674 pp., 2006. 667 Shi, Z., Song, C., Liu, B., Lu, G., Xu, J., Van Vu, T., Elliott, R. J. R., Li, W., Bloss, W. J., and 668 Harrison, R. M.: Abrupt but smaller than expected changes in surface air quality 669 attributable to COVID-19 lockdowns, Sci Adv, 7, 6696-6709, 670 https://doi.org/10.1126/SCIADV.ABD6696/SUPPL FILE/ABD6696 SM.PDF, 2021. Tian, J., Wang, Q., Zhang, Y., Yan, M., Liu, H., Zhang, N., Ran, W., and Cao, J.: Impacts of 671 672 primary emissions and secondary aerosol formation on air pollution in an urban area of 673 lockdown, Environ China during the COVID-19 Int, 150, 106426, 674 https://doi.org/10.1016/j.envint.2021.106426, 2021.

675 Tobler, A. K., Skiba, A., Wang, D. S., Croteau, P., Styszko, K., Necki, J., Baltensperger, U., 676 Slowik, J. G., and Prévôt, A. S. H.: Improved chloride quantification in quadrupole 677 aerosol chemical speciation monitors (Q-ACSMs), Atmos Meas Tech, 13, 5293–5301, 678 https://doi.org/10.5194/amt-13-5293-2020, 2020. 679 Transport for London: Travel in London Report 13, 2020. 680 UK Health Security Agency (UKHSA): Statement on the differential toxicity of particulate 681 constituents, matter according to source or 682 https://www.gov.uk/government/publications/particulate-air-pollution-health-effects-683 of-exposure/statement-on-the-differential-toxicity-of-particulate-matter-according-to-684 source-or-constituents-2022, 27 July 2022. 685 Vasilakopoulou, C. N., Matrali, A., Skyllakou, K., Georgopoulou, M., Aktypis, A., Florou, K., 686 Kaltsonoudis, C., Siouti, E., Kostenidou, E., Błaziak, A., Nenes, A., Papagiannis, S., 687 Eleftheriadis, K., Patoulias, D., Kioutsioukis, I., and Pandis, S. N.: Rapid transformation 688 of wildfire emissions to harmful background aerosol, NPJ Clim Atmos Sci, 6, 218, 689 https://doi.org/10.1038/s41612-023-00544-7, 2023. 690 Via, M., Chen, G., Canonaco, F., Daellenbach, K. R., Chazeau, B., Chebaicheb, H., Jiang, J., 691 Keernik, H., Lin, C., Marchand, N., Marin, C., O'dowd, C., Ovadnevaite, J., Petit, J.-E., 692 Pikridas, M., Riffault, V., Sciare, J., Slowik, J. G., Simon, L., Vasilescu, J., Zhang, Y., 693 Favez, O., Prévôt, A. S. H., Alastuey, A., and Cruz Minguillón, M.: Rolling vs. seasonal 694 PMF: Real-world multi-site and synthetic dataset comparison, Atmos Meas Tech, 15, 695 https://doi.org/10.5194/amt-15-5479-2022, 2022. 696 Wei, Y., Qiu, X., Yazdi, M. D., Shtein, A., Shi, L., Yang, J., Peralta, A. A., Coull, B. A., and

Schwartz, J. D.: The Impact of Exposure Measurement Error on the Estimated

698 Concentration-Response Relationship between Long-Term Exposure to PM2.5 and 699 Mortality, Environ Health Perspect, 130, https://doi.org/10.1289/EHP10389, 2022. 700 Wei, Y., Feng, Y., Danesh Yazdi, M., Yin, K., Castro, E., Shtein, A., Oiu, X., Peralta, A. A., 701 Coull, B. A., Dominici, F., and Schwartz, J. D.: Exposure-response associations 702 between chronic exposure to fine particulate matter and risks of hospital admission for 703 major cardiovascular diseases: population based cohort study, BMJ, e076939, 704 https://doi.org/10.1136/bmj-2023-076939, 2024. World Health Organization: WHO global air quality guidelines. Particulate matter (PM2.5 and 705 706 PM10), ozone, nitrogen dioxide, sulfur dioxide and carbon monoxide., Geneva, 2021. 707 Wu, D., Zheng, H., Li, Q., Wang, S., Zhao, B., Jin, L., Lyu, R., Li, S., Liu, Y., Chen, X., Zhang, 708 F., Wu, Q., Liu, T., Jiang, J., Wang, L., Li, X., Chen, J., and Hao, J.: Achieving health-709 oriented air pollution control requires integrating unequal toxicities of industrial 710 particles, Nature Communications 2023 14:1, 14, 1–12, https://doi.org/10.1038/s41467-711 023-42089-6, 2023. 712 Xu, J., Ge, X., Zhang, X., Zhao, W., Zhang, R., and Zhang, Y.: COVID-19 Impact on the 713 Concentration and Composition of Submicron Particulate Matter in a Typical City of 714 Northwest China, Geophys Res Lett, 47, https://doi.org/10.1029/2020GL089035, 2020. 715 Yao, X. and Zhang, L.: Identifying decadal trends in deweathered concentrations of criteria air 716 pollutants in Canadian urban atmospheres with machine learning approaches, Atmos 717 Chem Phys, 24, 7773–7791, https://doi.org/10.5194/acp-24-7773-2024, 2024. 718 Zhang, Qi., Jimenez, J. L., Canagaratna, M. R., Allan, J. D., Coe, H., Ulbrich, I., Alfarra, M. 719 R., Takami, A., Middlebrook, A. M., Sun, Y. L., Dzepina, K., Dunlea, E., Docherty, K.,

DeCarlo, P. F., Salcedo, D., Onasch, T., Jayne, J. T., Miyoshi, T., Shimono, A.,

721	Hatakeyama, S., Takegawa, N., Kondo, Y., Schneider, J., Drewnick, F., Borrmann, S.,
722	Weimer, S., Demerjian, K., Williams, P., Bower, K., Bahreini, R., Cottrell, L., Griffin,
723	R. J., Rautiainen, J., Sun, J. Y., Zhang, Y. M., and Worsnop, D. R.: Ubiquity and
724	dominance of oxygenated species in organic aerosols in anthropogenically-influenced
725	Northern Hemisphere midlatitudes, Geophys Res Lett, 34, n/a-n/a,
726	https://doi.org/10.1029/2007GL029979, 2007.